RSC Advances

COMMUNICATION

View Article Online
View Journal | View Issue

Cite this: *RSC Adv.*, 2015, **5**, 77734

Received 10th July 2015
Accepted 7th September 2015

DOI: 10.1039/c5ra13552d

www.rsc.org/advances

Genetically encoded phenyl azide photochemistry drives positive and negative functional modulation of a red fluorescent protein†‡

Samuel C. Reddington,§[a] Sarunas Driezis,§[a] Andrew M. Hartley,§[a] Peter D. Watson,[a] Pierre J. Rizkallah[b] and D. Dafydd Jones*[a]

The photochemical properties of phenyl azide have been exploited to modulate the function of a red autofluorescent protein, mCherry. Using genetic code reprogramming, phenyl azide chemistry has been introduced at functionally strategic positions in mCherry leading to deactivation, activation or enhancement upon UV irradiation.

Optical control of biological processes whereby light is used to modulate inherent protein function is fast becoming an important tool in the biosciences as a means to precisely control protein activity with high temporal and spatial resolution not achievable through classical transcriptional control.[1–3] Existing approaches to genetically encode protein photocontrol, known as optogenetics, generally utilise versions of natural light sensing proteins that detect and respond to light through the use of non-proteinaceous cofactors (*e.g.* retinal and flavins). The main drawback is the requirement for whole protein domains (*e.g.* LOV domains[4] or membrane bound opsins[2]) to encode the light-responsive properties. An alternative approach is to use photoreactive chemical groups that can be programmed directly into a protein through the use of non-canonical amino acids (ncAAs).[5] One such ncAA, *p*-azido-phenylalanine (azF; Fig. 1a), is particularly useful as it has a relatively small side-chain compared to other ncAAs (N_3 at the *para* position instead of OH in the natural amino acid tyrosine) and can easily be photoconverted to a highly reactive nitrene radical (Fig. 1a).[6,7] Subsequent products of the various nitrene reaction pathways can be used to alter protein structure and thus control function.[8]

Autofluorescent proteins are unique in nature in that they absorb and emit light in the visible range without the requirement of cofactors.[9,10] Contiguous amino acids within the core of the protein covalently rearrange in the presence of O_2 to form an extended conjugated π system that acts as a chromophore. Photoresponsive versions of autofluorescent proteins are critical to modern super-resolution microscopy.[11] The two main classes of autofluorescent proteins are the green[10] (primarily derived from the classical *Aequorea victoria* GFP) and red[9] (primarily derived from the oligomeric

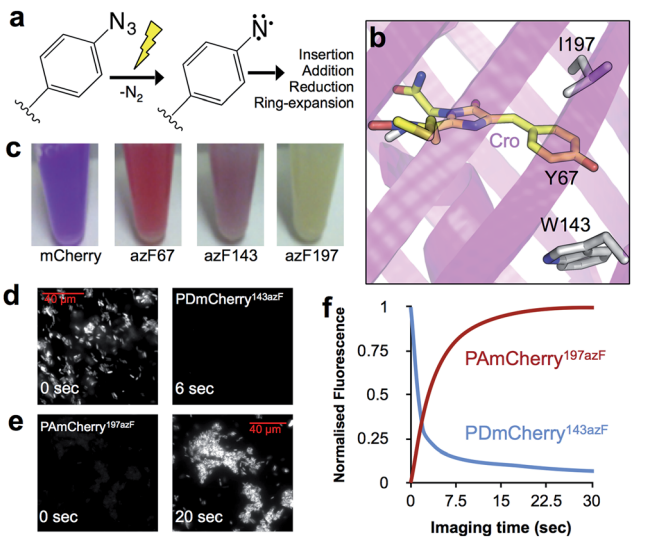

Fig. 1 Incorporation of phenyl azide chemistry into mCherry. (a) Side chain and photochemical properties of *p*-azido-L-phenylalanine (azF). (b) Selected residues in mCherry where azF incorporation instilled photochemical control on the protein. (c) The effect of azF incorporation at the selected residues in mCherry on the transmissive colour. (d) Photodeactivation of PDmCherry^{143azF} and (e) photoactivation of PAmCherry^{197azF} in live cells after UV irradiation at 350 nm. (f) Change in live cell fluorescence over time for PDmCherry^{143azF} and PAmCherry^{197azF} on irradiation at 350 nm. Live cell imaging was performed using widefield microscopy.

[a]*School of Biosciences, Cardiff University, Cardiff, UK. E-mail: jonesdd@cardiff.ac.uk; Tel: +44 (0)2920 20874290*

[b]*School of Medicine, Cardiff University, Cardiff, UK*

† The PDB accession codes for dark and irradiated PDmCherry^{143azF} are 4ZIN and 4ZIO. We would like to thank the staff at the Diamond Light Source for the supply of facilities and beam time, especially Beamline I03 and I04 staff. We thank BBSRC (BB/H003746/1 and BB/M000249/1), EPSRC (EP/J015318/1) and Cardiff SynBio Initiative/SynBioCite for supporting this work.

‡ Electronic supplementary information (ESI) available: Detailed methods, supporting Fig. S1–S7, supporting Tables S1–S3. See DOI: 10.1039/c5ra13552d

§ All these authors contributed equally to this work.

Discosoma sp. DsRed) versions. While the two protein classes share a common β-can structure, their sequence identities are low with distinct chromophore structures, maturation and environment; all these factors contribute towards the significant differences in fluorescence between these autofluorescent proteins. Thus, useful mutations cannot always be simply transferred to the other. Red autofluorescent proteins are becoming the preferred option in cell imaging due to their lower excitation wavelength energy and reduced inherent cellular fluorescence background. While previous efforts have highlighted how ncAAs,[12] including azF,[13,14] can influence the properties of GFPs, little is known about their potential impact and use with respect to red versions. Here we address this using the widely used DsRed variant mCherry[15] and show by replacing single pre-selected residues with azF how function can be either positively or negatively regulated by UV irradiation, both *in vitro* and *in vivo*.

Based on analysis of the mCherry structure [PDB 2H5Q[16]], residues in and around the chromophore were selected for replacement with azF (Fig. 1b and S1‡). Of the twelve different mutants generated, ten were produced as soluble protein, suggesting incorporation of azF within the protein core did not impact protein folding (Table S1‡). All but two of the soluble variants had a measureable fluorescent signal before and/or after UV irradiation, suggesting that azF is functionally tolerated within the core of the protein. On UV irradiation, fluorescence changes varied depending on the placement of azF and included decreases, increases and/or shifts in λ_{EX} and λ_{EM} (Table S1‡). While mCherry itself has a degree of sensitivity to UV light (Table S1 and Fig. S2‡), most of the photoresponsive azF mutants displayed a significantly greater magnitude of change. Three variants (Y67azF, W143azF and I197azF; Fig. 1b) exhibited the largest fold change in fluorescence and were selected for further characterisation.

Replacement of W143 with azF (termed PDmCherry^{143azF}, where PD refers to photodeactivation) generated a highly fluorescent protein in its dark state (pre-irradiation) that was responsive to UV light. Prior to irradiation, widefield microscopy of live *E. coli* cells indicated that PDmCherry^{143azF} was relatively stable to photobleaching with a $t_{1/2}$ of 76 s at 555 nm under typical imaging conditions for mCherry. The spectral peaks were slightly blue shifted (2–5 nm) compared to mCherry and it had a 20% lower quantum yield (Φ) and ~50% lower molar extinction coefficient (ε) (Table 1). PDmCherry^{143azF} was very sensitive to UV light (Fig. 1d), with live cell imaging revealing irradiation at 350 nm rapidly decreased observed fluorescence beyond the level inherent to mCherry (Fig. S2‡) with a $t_{1/2}$ of 10 s. Detailed *in vitro* analysis confirmed these findings with PDmCherry^{143azF} converting to a form with low fluorescence (Fig. 2a and Table 1). The absorbance spectrum indicated that photolysed protein still retained an entity that acts as a chromophore (λ_{max} 582 nm), albeit with a slightly lower extinction coefficient (Fig. 2b).

To investigate the potential mechanism of action, the crystal structures of PDmCherry^{143azF} resolved to 1.7 Å (dark; PDB code 4ZIN) and 2.0 Å (light; PDB code 4ZIO) were determined (see ESI for details‡). The structure of the dark state revealed that the

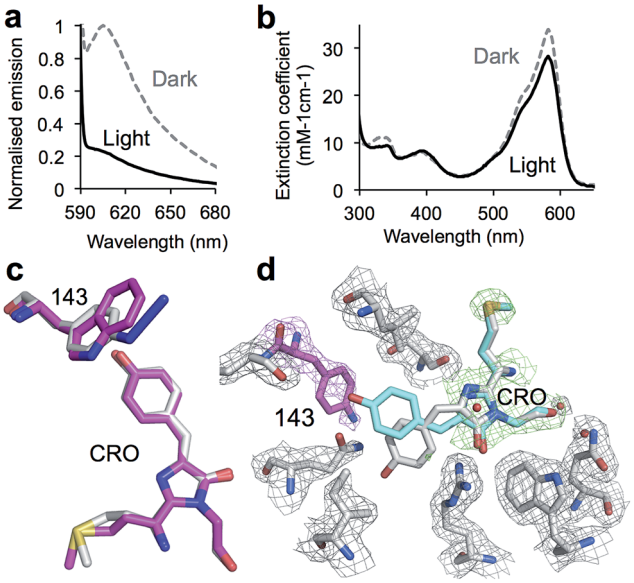

Fig. 2 Photodeactivation properties of PDmCherry^{143azF}. (a) Fluorescence emission spectra (on excitation at 584 nm) and (b) corresponding absorbance spectra of protein before (dark; grey dashed line) and after (light; black line) UV irradiation (60 min). (c) Crystal structure of the dark state PDmCherry^{143azF} (carbons coloured grey) compared to mCherry structure (carbons coloured magenta) highlighting the chromophore (CRO) and residue 143. (d) The structure of the light state PDmCherry^{143azF} with the electron density maps of CRO (grey/cyan), residue 143 (magenta) together with surrounding residues (grey) shown. Potential conformations for CRO are modelled in.

Table 1 Spectral properties of purified mCherry^{azF} variants

Variant	λ_{max} (nm)	λ_{EX} (nm)	λ_{EM} (nm)	State	ε (M^{-1} cm^{-1})	Φ	Brightness M^{-1} cm^{-1}	Fold change[a]
PDmCherry^{W143azF}	582	584	608	Dark	34 000	0.18	6120	5.1
				UV[b]	25 800	0.06	1548	
PAmCherry^{I197azF}	584	587	610	Dark	<1000	ND[c]	—	≥14.1
				UV[b]	11 600	0.05	580	
mCherry[d]	587	587	610	—	72 000	0.22	15 840	—

[a] Fold change in fluorescence of variants was calculated from *in vitro* fluorescence spectra before and after photolysis. [b] Irradiated using a 5 W handheld lamp. [c] ND = not determined. The quantum yield of PAmCherry^{I197azF} before photolysis was too low to be determined as protein absorbance (ε) was too low. [d] From N. C. Shaner, *et al.*, *Nat. Biotechnol.*, 2004, 22, 1567–1572.

variant has an essentially identical structure to mCherry with both the chromophore and residues at 143 occupying similar positions and planes (Fig. 2c). The packing around the chromophore was also very similar (Fig. S3‡). Thus, inserting a phenyl azide moiety into the core of the protein did not significantly disrupt structure. However, the presence of the azide group with its inherent resonance structures close to the chromophore may be influencing the latter's electronic properties.

Residue 143 lies close to the chromophore in mCherry (and the W143azF variant; Fig. 2c), occupying an equivalent position to Y/F145 in GFP, but both the backbone and the side chain placements differ significantly between the two (Fig. S4‡). Replacement of F145 in superfolder GFP (sfGFP[17]) with azF also led to loss of fluorescence on irradiation[14] but by a different mechanism; the phenyl nitrene forms a crosslink to the chromophore so restricting chromophore mobility and reducing the extended conjugated double bond system. In contrast, the structure of irradiated PDmCherry^{143azF} strongly suggests increased chromophore mobility is causing loss of fluorescence (Fig. 2d) with little change to the chromophore structure (Fig. 2b). The electron density for the irradiated form was generally poor over the chromophore region and residue 143, with no electron density observed for the *p*-hydroxybenzylidene chromophore moiety (Fig. 2d). The most likely explanation is the absence of a single defined conformation of the chromophore in the crystal, which suggests conformational flux of the chromophore upon UV irradiation of PDmCherry^{143azF}. Isomerism and bond angle changes involving the chromophore are known to influence fluorescence.[11] Indeed, the hydroxybenzylidene can be modeled to both the *cis* and *trans* conformation without steric problems or overlap with observed electron density (Fig. 2d). The limited electron density observed for residue 143 suggests a single atom protrusion at the *para* position, which we have tentatively assigned as the phenyl amine product of azF photolysis (Fig. 2d). The side chain of residue 143 points away from the chromophore, with the likely position of the nitrene radical being too far away (5.5–6 Å) to form a crosslink with the chromophore (Fig. 2d). The similar absorbance spectra for both dark and light forms of PDmCherry^{143azF} suggest that the chemical structure is not significantly perturbed on irradiation. Otherwise, the structures of the dark and light states are very similar (Fig. S3‡) highlighting the crucial role relatively small structural changes instigated by azF photochemistry have on modulating fluorescent protein function and local dynamics.

Replacement of I197 with azF resulted in the production of a non-fluorescent protein (termed PAmCherry^{197azF}, where PA refers to photoactivation) with little inherent colour (Fig. 1c), cellular fluorescence (Fig. 1d) or absorbance (Fig. 3a). Neither the Φ nor ε for the non-irradiated form could be accurately calculated, suggesting that chromophore maturation had been impeded on production of the protein in the dark. Live cell imaging by widefield microscopy revealed that PAmCherry^{197azF} could be rapidly activated by UV irradiation, with an observed $t_{1/2}$ at 350 nm of 10 s (Fig. 1d). UV irradiated PAmCherry^{197azF} showed higher apparent photostability than native mCherry, a key characteristic of photoactivatable fluorescent proteins (compare Fig. 1f and S2b‡); no apparent decrease in cellular fluorescence was observed after 60 s of imaging. More detailed *in vitro* studies demonstrated that on irradiation, fluorescence increased ~14 fold in intensity with a final λ_{EX} and λ_{EM} similar to mCherry (Fig. 3a and Table 1). While irradiation resulted in functional activation, presumably through inducing chromophore maturation, the irradiated protein was less bright than native mCherry (Table 1) but could still imaged by microscopy (Fig. 1e).

I197 lies just above the plane of the chromophore in mCherry at an equivalent structural position to T203 in GFP (Fig. S5‡). Together with numerous additional mutations, substitution of I197 (to arginine) has previously contributed towards the generation of useful photoactivatable mCherry variants.[18] In contrast to the observations here for PAmCherry^{I197azF}, replacement of T203 in sfGFP with azF did not appear to significantly affect chromophore maturation but did red shift excitation and emission in the dark.[13] The absence here of a red shift in spectral properties suggests that PAmCherry^{197azF} does not display aromatic stacking between residue 197 and the chromophore. Also, photolysis of sfGFP T203azF results in a major reduction in extinction coefficient (~5 fold)[13] whereas substantial increase is observed for PAmCherry^{I197azF} (Table 1). Thus, in this case the influence of azF and its photochemistry on function is not simply transferred from sfGFP to mCherry highlighting the role played by the local chemical environment.

I197 together with K70 are known to have an important role in chromophore maturation in mCherry,[19] especially concerning the Y67 Cα–Cβ oxidation step, with K70 acting as a general base for proton abstraction.[20] Given the proximity of K70 and I197 in space (Fig. S5‡), replacement of residue 197 is likely to disrupt the positioning of K70, so preventing it from acting as a general base. It is now thought that chromophore maturation of DsRed derived proteins (such as mCherry) proceed *via* a blue emitting intermediate, equivalent to the conjugated imidazolinone and acylimine groups.[19,20] Loss of the potential Cα–Cβ oxidation step does not explain the apparent lack of this intermediate form in the dark state. This suggests that prior to irradiation, chromophore maturation progresses to, at most, the formation of the initial cyclised non-oxidised form

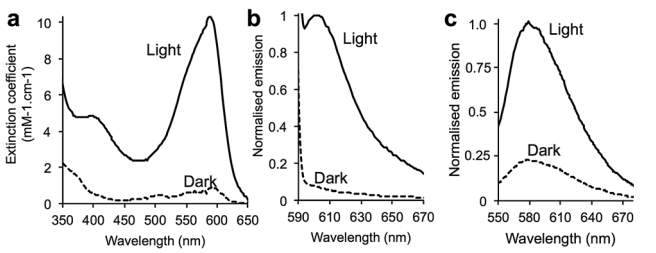

Fig. 3 Photoactivating mCherry azF variants. (a) Absorbance and (b) fluorescence emission (excited at 587 nm) spectra of PAmCherry^{197azF} before (dark) and after (light) UV irradiation. (c) The emission spectra of PEmCherry^{67azF} on excitation at 541 nm before (dark) and after (light) UV irradiation.

(through the linking of residues M66 and G68). One hypothesis is that the phenyl azide group alters the positions of key residues such as K70 involved in chromophore maturation at both the Y67 Cα–Cβ and the M66 N–Cα oxidation steps required for a completed conjugation system. It could be possible that loss of molecular N_2 (and associated local structural rearrangements) together with the formation of the nitrene radical itself and/or a final reaction product (*e.g.* phenyl amine) is involved in the maturation pathway, substituting for or modulating the role played by residues such as K70 in mCherry. Unfortunately, we were unable to crystallise this variant. It is important to note that it is the azide moiety that is likely to play the key role in controlling maturation in PAmCherry^{197azF} as mutation to tyrosine (I197Y mutant) does not affect mCherry maturation fluorescence (Fig. S6‡).

The mCherry Y67azF variant (equivalent to Y66 in GFP), termed PEmCherry^{67azF} (where PE refers to photoenhancement), has the tyrosine within the chromophore replaced. The transmissive properties of PEmCherry^{67azF} were very different to mCherry with cell lysates turning from a purple to red colour (Fig. 1c), with replacement of the phenol group with phenyl azide in the chromophore the likely cause (*vide infra*). PEmCherry^{67azF} was produced as a weakly fluorescent protein with the emission peak blue shifted by ~50 nm compared to mCherry (Table S1‡), which is in keeping with previous observations that the electron rich azido group can act as a fluorescence quencher.[8,21] On UV irradiation with low power UV light, a 3.4 fold increase in fluorescence was observed, with the blue shift in λ_{EX} and λ_{EM} compared to mCherry retained (Fig. 3b and Table S1‡). Previous work with GFP suggests that this is caused by the conversion of the phenyl azide to a phenyl amine.[14] Replacing azF at residue 67 with *p*-amino-L-phenylalanine to mimic the potential photochemical endpoint produced a protein with similar maximal excitation and emission wavelengths to that of the irradiated PEmCherry^{67azF} (Fig. S7‡), supporting the idea of conversion to the phenyl amine. The exchange of the phenol, or more accurately phenolate to phenyl amine changes the electron donation strength of the aromatic component and thus the resonant structures of the chromophore. This in turn could cause the observed blue shift in fluorescence.

The genetic incorporation of phenyl azide chemistry into proteins is a potentially general tool for controlling protein activity through the use of light without the need for bulky protein domains and additional cofactors. As demonstrated here with the widely used autofluorescent protein mCherry, the position within the protein's molecular structure is critical to how the potential photochemical pathway taken will ultimately impact function. Through incorporation of a single ncAA at three disparate positions in the protein core, we have generated PD, PA and PE mCherry variants, that could be developed into useful tools for microscopy. FRAP (fluorescence recovery after photobleaching) microscopy[22] is normally hindered by the photostability of autofluorescent proteins meaning long and relatively intense illumination are required to deactivate the protein. This results in the loss of temporal resolution. PDmCherry^{143azF} is relatively photostable at imaging wavelengths but can be rapidly deactivated at low light energy making it potentially an excellent probe for furthering FRAP microscopy. PALM (photoactivated localisation microscopy) requires photoactivatable fluorescent proteins with high levels of photostability,[23,24] a characteristic we have successfully introduced into PAmCherry^{197azF}. While photocontrol of autofluorescent proteins (including mCherry[18]) require multiple canonical mutations to achieve useful light-sensitive properties, we have shown here that incorporation of a single light sensitive ncAA can achieve a similar endpoint and sample different photochemical effects. Improved approaches for efficient and higher yielding ncAAs containing proteins in different cells and organisms[25] combined with the inherent chemical genetic element (ncAA-dependent protein production) will broaden the potential use with regards to autofluorescent proteins and proteins in general.

Notes and references

1 K. Deisseroth, *Nat. Methods*, 2011, **8**, 26–29.
2 A. Gautier, C. Gauron, M. Volovitch, D. Bensimon, L. Jullien and S. Vriz, *Nat. Chem. Biol.*, 2014, **10**, 533–541.
3 J. E. Toettcher, C. A. Voigt, O. D. Weiner and W. A. Lim, *Nat. Methods*, 2011, **8**, 35–38.
4 A. Moglich and K. Moffat, *Photochem. Photobiol. Sci.*, 2010, **9**, 1286–1300.
5 A. Gautier, A. Deiters and J. W. Chin, *J. Am. Chem. Soc.*, 2011, **133**, 2124–2127.
6 J. Chin, S. Santoro, A. Martin, D. King, L. Wang and P. Schultz, *J. Am. Chem. Soc.*, 2002, **124**, 9026–9027.
7 S. Reddington, P. Watson, P. Rizkallah, E. Tippmann and D. D. Jones, *Biochem. Soc. Trans.*, 2013, **41**, 1177–1182.
8 J. L. Morris, S. C. Reddington, D. M. Murphy, D. D. Jones, J. A. Platts and E. M. Tippmann, *Org. Lett.*, 2013, **15**, 728–731.
9 A. Miyawaki, D. M. Shcherbakova and V. V. Verkhusha, *Curr. Opin. Struct. Biol.*, 2012, **22**, 679–688.
10 R. Y. Tsien, *Annu. Rev. Biochem.*, 1998, **67**, 509–544.
11 D. M. Shcherbakova and V. V. Verkhusha, *Curr. Opin. Chem. Biol.*, 2014, **20**, 60–68.
12 W. Niu and J. Guo, *Mol. BioSyst.*, 2013, **9**, 2961–2970.
13 S. C. Reddington, A. J. Baldwin, R. Thompson, A. Brancale, E. M. Tippmann and D. D. Jones, *Chem. Sci.*, 2015, **6**, 1159–1166.
14 S. C. Reddington, P. J. Rizkallah, P. D. Watson, R. Pearson, E. M. Tippmann and D. D. Jones, *Angew. Chem., Int. Ed.*, 2013, **52**, 5974–5977.
15 N. C. Shaner, R. E. Campbell, P. A. Steinbach, B. N. Giepmans, A. E. Palmer and R. Y. Tsien, *Nat. Biotechnol.*, 2004, **22**, 1567–1572.
16 X. Shu, N. C. Shaner, C. A. Yarbrough, R. Y. Tsien and S. J. Remington, *Biochemistry*, 2006, **45**, 9639–9647.
17 J. D. Pedelacq, S. Cabantous, T. Tran, T. C. Terwilliger and G. S. Waldo, *Nat. Biotechnol.*, 2006, **24**, 79–88.
18 F. V. Subach, G. H. Patterson, S. Manley, J. M. Gillette, J. Lippincott-Schwartz and V. V. Verkhusha, *Nat. Methods*, 2009, **6**, 153–159.

19 F. V. Subach, V. N. Malashkevich, W. D. Zencheck, H. Xiao, G. S. Filonov, S. C. Almo and V. V. Verkhusha, *Proc. Natl. Acad. Sci. U. S. A.*, 2009, **106**, 21097–21102.
20 F. V. Subach and V. V. Verkhusha, *Chem. Rev.*, 2012, **112**, 4308–4327.
21 K. Sivakumar, F. Xie, B. M. Cash, S. Long, H. N. Barnhill and Q. Wang, *Org. Lett.*, 2004, **6**, 4603–4606.
22 A. Miyawaki, *Nat. Biotechnol.*, 2004, **22**, 1374–1376.
23 M. Fernandez-Suarez and A. Y. Ting, *Nat. Rev. Mol. Cell Biol.*, 2008, **9**, 929–943.
24 J. Lippincott-Schwartz and G. H. Patterson, *Trends Cell Biol.*, 2009, **19**, 555–565.
25 J. W. Chin, *Annu. Rev. Biochem.*, 2014, **83**, 379–408.